Wear 267 (2009) 653–660

Contents lists available at ScienceDirect

Wear

journal homepage: www.elsevier.com/locate/wear

A route to wear resistant PTFE via trace loadings of functionalized nanofillers

D.L. Burris[a,*], S. Zhao[b], R. Duncan[b], J. Lowitz[c], S.S. Perry[c], L.S. Schadler[b], W.G. Sawyer[c]

[a] University of Delaware, Newark, DE, USA
[b] Rensselaer Polytechnic Institute, Troy, NY, USA
[c] University of Florida, Gainesville, FL, USA

ARTICLE INFO

Article history:
Received 7 August 2008
Received in revised form 17 December 2008
Accepted 17 December 2008

Keywords:
Nanocomposite
Dispersion
Interface
Polytetrafluoroethylene
Space
Solid lubrication

ABSTRACT

A fluorosilane nanoparticle surface treatment of alumina nanoparticles was studied to test a hypothesis that reduced surface energy would improve dispersion and extend wear resistance of polytetrafluoroethylene (PTFE) to trace nanoparticle loadings. Dry sliding wear tests were performed on PTFE nanocomposites with 0.00, 0.13, 0.50 and 1.00% untreated and treated 40 nm α phase alumina nanoparticles. The untreated alumina reduced the wear of PTFE by 10–100× at 0.13% loading with variability typical of lightly loaded PTFE nanocomposites. The treated nanoparticles reduced the wear of PTFE by 6000× at 0.13% loading and demonstrated no evidence of variability; wear was improved 6000–10,000× with 0.13–1% nanoparticle loading. AFM morphology studies revealed that the α phase alumina nanoparticles altered the PTFE morphology. Correlation between PTFE wear resistance and morphology was demonstrated as far less effective δ:γ phase alumina had no appreciable effect on PTFE morphology. During TEM dispersion characterization, the untreated nanoparticles were found primarily in clusters while treated nanoparticles were found individually dispersed. It is believed that the surface properties of the α phase particles induce a wear resistant PTFE morphology, while the fluorosilane treatment facilitated dispersion and extended the beneficial effects of the nanoparticles to significantly lower loadings.

1. Introduction

Polytetrafluoroethylene (PTFE) is a low friction, high temperature, chemically inert and biocompatible material. This unique combination of properties makes PTFE indispensible in a number of extreme applications. Unfortunately, its application as an extreme environment solid lubricant has been preclude by a prohibitively high wear rate [1–4]. Numerous hard fillers can abate severe wear of PTFE, but typically this comes at the expense of its other beneficial properties (most notably friction) [1,2,5–8].

Even small weight percents of nanofillers can have high number densities and surface areas, and as a result, they have unique and well-documented potential for modifying certain properties of a polymer matrix with very low loadings (0.1–5%) [9–12]. Tanaka and Kawakami tested nanoscale TiO_2 against other traditional fillers in a PTFE matrix for novel improvements in performance [8]. The poor relative performance of the nanofiller in this study led to a prevailing sentiment that nanofillers are too small to interfere with the large-scale processes associated with PTFE wear. Starting in 2001, three independent studies on the effect of nanoparticle loading on PTFE wear were published using ZnO, carbon nanotubes (CNT) and alumina [13–15]. The results of these studies, shown in Fig. 1, show remarkably similar trends; 10× wear reductions near 1% and 100–1000× reductions at the optimum which occurred above 10%. The requirement for high loading and material independence suggest that the wear reduction mechanism is largely due to a mechanical effect of the nanoparticles. In direct contrast, however, a 2005 study by Burris and Sawyer revealed the first evidence of a nanoscale-specific wear resistance mechanism; α alumina-PTFE was more than 100× more wear resistant than prior nanocomposites (including its δ:γ alumina counterpart) at loadings below 5% [16,17]. McElwain confirmed the unique effects of α alumina at 2.5%, but found almost no improvement in wear at 0.4% [6,18].

The mechanisms responsible for many of these observations remain poorly understood; to date, only α phase alumina has induced low wear in PTFE at low loadings [6,16–18]. Recent studies suggest that low wear at low nanoparticle loadings requires several synergistic factors acting simultaneously [19]:

(1) Nanoparticle modification of the crystalline morphology. While traditional fillers largely act as mechanical reinforcements by supporting load, initiating crazes and interrupting crack propagation, nanofillers are of the same size scale as polymer lamellae and can alter the crystalline morphology of the matrix. Changes in the crystalline morphology can lead to large changes in a variety of physical properties [20–26]. Unusual fibrillation of the

* Corresponding author. Tel.: +1 302 831 2006.
E-mail address: dlburris@udel.edu (D.L. Burris).

0043-1648/$ – see front matter © 2009 Elsevier B.V. All rights reserved.
doi:10.1016/j.wear.2008.12.116

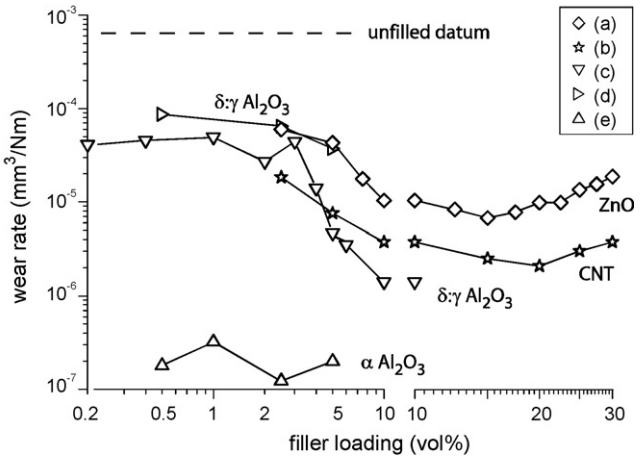

Fig. 1. Review of PTFE nanocomposites wear literature with wear rate plotted versus filler loading (vol%): (a) Li et al. [14], (b) Chen et al. [13], (c) Sawyer et al. [15], (d) Burris and Sawyer [16], Burris and Sawyer [17]. Until 2006, the PTFE nanocomposites in the literature demonstrated consistent trends, namely, notable reductions (~10×) in wear rate with trace loadings (<1%) and further reductions (approaching 1000×) up to an optimum loading around 10–20% nanofiller. This consistency suggested material and process insensitivity. In 2006, Burris and Sawyer found that a particular phase of alumina induced unusual wear resistance in PTFE at unprecedented low loadings.

matrix during wear and tensile testing suggest such a change in the crystalline morphology of low wear PTFE [19,27,28].

(2) Reduced abrasion. One of the most critical benefits of the small filler size is low abrasiveness as compared to more traditional hard fillers such as glass fibers and microscale particles. In a manner analogous to polishing with fine grit, nanofillers polish the highest asperities with very low material removal rates, and prepare the surface for transfer film initiation.

(3) Stable transfer films. When subsurface damage is restricted, fibrillation at the surface produces thin, well adhered transfer films that develop without interruption by large abrasive fillers. These transfer films play several essential roles; they provide a low shear strength interface, they protect the nanocomposite from the counterface and they protect the counterface from the abrasive filler [29]. In the case of PTFE, the longevity of the transfer film leads to defluorination, and the formation of a very wear resistant chemically and mechanically altered polymer surface coating [19].

It remains unclear how or why these particles initiate the above mechanisms. It is hypothesized that the PTFE has a unique response to the structure or chemistry of the nanoparticle. In this model, the spatial density of the nanoparticles within the matrix (dispersion) determines the effective influence of these nanoscopic interactions over the macroscopic lengths of the part. In this paper, we varied dispersion by reducing nanoparticle surface energy with a fluorinated silane (hereafter referred to as fluorosilane) surface treatment. Treated and untreated α alumina-PTFE nanocomposites of 0.00, 0.13, 0.50 and 1.00% loadings were created and tested to study the effects of the particles and their dispersion characteristics on the wear resistance of PTFE.

2. Experimental methods

2.1. Materials and processing

The solid lubricant matrix used in this study is a virgin polytetrafluoroethylene molding resin (Teflon 7C from DuPont – 30 μm particles). The nanofiller material is 40 nm α phase alumina from Alfa Aesar; TEM imaging suggests an average size of around 20 nm. Nanocomposites with 0.00, 0.13, 0.50 and 1.00% (by volume) alumina loading were processed and tested. In the untreated group, the nanoparticles were dispersed as received; two identical sets were created to test the role of dispersion on variability. In the treated group, nanoparticles were given a fluorosilane surface treatment. These nanoparticles were chemically treated with 3,3,3 trifluoropropyl trimethoxysilane: 2 g of nanoscale alumina was added to 50 ml of ethanol with 2.5 g deionized water. A wand sonicator was used to break up nanoparticle agglomerates. After 5 min of sonication, 3 g of silane was added and sonication was continued for another 10 min. The reflux reaction was carried out at 80 °C in an oil bath for three days. The nanoparticles were separated from the solution by centrifuging. Both ethanol and hexane were used consecutively to wash away any excess silane. Following the washing procedure, the nanoparticles were subjected to vacuum drying at 25 °C. Infrared spectroscopy confirmed the presence of the fluorinated treatment and thermal gravimetric analysis (TGA) provided a treatment mass fraction of approximately 3%. Following the treatment, the silanol chains are bound to the alumina and terminated with groups of CF_3.

Nanocomposite processing was achieved through the mixing, dispersion and compression molding techniques described in Sawyer et al. [15]. Briefly, appropriate proportions of the powders were hand-mixed to achieve gross homogeneity. This powder ensemble was then fed into a jet-mill, which is an open device that uses a high energy air-jet to accelerate, grind, classify and cool the particles. As the powders enter the grinding chamber of the jet-mill, the particles impact each other, disbanding agglomerates and dispersing the particles. Thermal gravimetric analysis (TGA) by Sawyer et al. [15] with higher loadings showed that about 60% of the fine nanoparticles are lost during jet-milling. Because TGA is insensitive to the loadings used here, we have corrected our loadings to 40% the pre-blended loading. The powders were jet-milled three times before compression molding at 362 °C. The stability limit of the fluorosilane is 200 °C. During compression molding, the surface coating is completely volatilized to eliminate the potentially confounding effects of the coating on the interface interactions. After molding, the final 6.3 mm × 6.3 mm × 12.7 mm tribology specimen was machined from the 12.7 mm diameter × 38 mm long molded puck using computer numerical control for repeatability. The counterfaces used in this study were 304 stainless steel flats with a lapped surface finish of 150 nm average roughness. Additional details of this surface can be found in Burris and Sawyer [16]. Three neat PTFE control samples were identically prepared and tested.

2.2. Tribology characterization

A laboratory designed linear reciprocating tribometer was used to test the wear and friction of the samples; this testing apparatus and the uncertainties associated with the experimental measurements are described in detail in Schmitz et al. [30,31]. Although open to the air, the entire apparatus was located inside a soft-walled cleanroom with conditioned laboratory air of relative humidity between 25% and 50%. The composite samples were mounted directly to a 6-channel load cell and the counterface was mounted to a linear reciprocating stage. Prior to testing, the counterfaces were washed in soap and water, cleaned with acetone, sonicated for ~15 min in methanol, and dried with a laboratory wipe. After dry machining, the composite samples were wiped clean with methanol.

A normal force of 250 N was applied via a pneumatic cylinder/linear thruster assembly, which results in a nominal contact pressure of 6.3 MPa over the 6.3 mm × 6.3 mm contact area. The load was continuously monitored and feedback controlled using an electro-pneumatic valve. The reciprocating length was 25.4 mm and the nominally constant sliding speed is 50.8 mm/s.

Table 1
Tribological results of 40 nm α alumina-PTFE nanocomposites. Normal load was 250 N, contact pressure was 6.4 MPa and sliding speed was 50.8 mm/s. The experimental uncertainty in wear rate is calculated according to the uncertainty analysis presented in Schmitz et al. [25]. The standard deviation in friction coefficient is calculated from time averaged values collected throughout testing; the uncertainty is $U_c(\mu) = 0.005$.

Alumina (vol%)	Alumina treatment	Steady wear rate (k) ($\times 10^{-6}$ mm^3/N m)	$U_c(k)$ ($\times 10^{-6}$ mm^3/N m)	μ	$\sigma(\mu)$
0.00	N/A	493	2.20	0.119	0.004
0.00	N/A	593	2.96	0.119	0.007
0.00	N/A	418	2.19	0.116	0.011
0.13	Untreated	29.0	0.110	0.190	0.012
0.13	Untreated	3.70	0.014	0.194	0.023
0.13	Treated	0.11	0.001	0.174	0.019
0.50	Untreated	0.06	0.001	0.175	0.017
0.50	Untreated	0.48	0.006	0.165	0.015
0.50	Treated	0.08	0.001	0.215	0.020
1.00	Untreated	0.60	0.002	0.174	0.012
1.00	Untreated	1.00	0.006	0.178	0.014
1.00	Treated	0.07	0.001	0.210	0.023

Interrupted mass measurements were made periodically throughout the test to quantify wear; this technique was used in place of the more typical pin displacement techniques that are confounded by sample creep and thermal expansion. Steady state wear rates and uncertainties are reported in this study following techniques discussed in Schmitz et al. [30]. The confidence intervals on wear rate data represent the experimental uncertainties in the measurements while the confidence intervals on friction coefficient data represent the standard deviations in friction coefficients. The uncertainty in friction coefficient is less than $U_c(\mu) = 0.005$ [31].

2.3. Morphology characterization

Portions of the samples were embedded into an epoxy mixture and cured for 24 h at 60 °C for morphology and dispersion studies. The embedding mixture comprised Embed 812, Araldite, DDSA and DMP30. For the PTFE morphology studies, the specimens were microtomed to a thickness approximating 200 nm using a RMC Product Ultra Microtome MTXL machine by Boeckler.

Potential morphological changes of the PTFE that resulted from nanoparticle inclusion were probed with an Asylum Research MFP-3D atomic force microscope (AFM) in AC tapping mode. Phase images were collected using a silicon tip (Nanoworld ArrowNC) with a measured resonant frequency of 283.3 kHz and a nominal tip radius of curvature less than 10 nm. Regions of interest on the microtomed and annealed samples were identified using an integrated optical microscope and were aligned to the tip with the instrument's motorized x–y positioning stage. Images of 512 × 512 pixels were collected at a scanning frequency of 0.6 Hz.

2.4. Dispersion characterization

For the dispersion studies, the specimens were microtomed to ~100 nm using a RMC CRX cryogenic system; PTFE is notoriously difficult to section uniformly and liquid nitrogen was needed to produce useful samples for TEM imaging. Transmission electron microscopy (TEM, Phillips CM12) was employed to image the dispersion of nanoparticles at an accelerating voltage of 120 kV. The images of the nanocomposite sections were analyzed and the locations of the nanoparticles were identified.

There remains no standard for nanoparticle dispersion characterization. Typically, dispersion is qualitatively illustrated using a representative TEM image. These distributions are incredibly complicated and require an enormous number of statistical parameters for accurate representation. Here, we make no effort to quantify dispersion; rather the size of the regions not occupied by nanoparticles is of primary importance to our hypothesis. The larger these unreinforced regions, the lower the probability that all of the PTFE will be affected by the interfaces. The method used here provides a quantitative single parameter measure of this length; it directly probes our hypothesis, it is simple and it is physically intuitive. The basic procedure was presented previously by Burris et al. [28] and is similar in its mechanics to the radial distribution function method [32], with the very important distinction that the length scale of

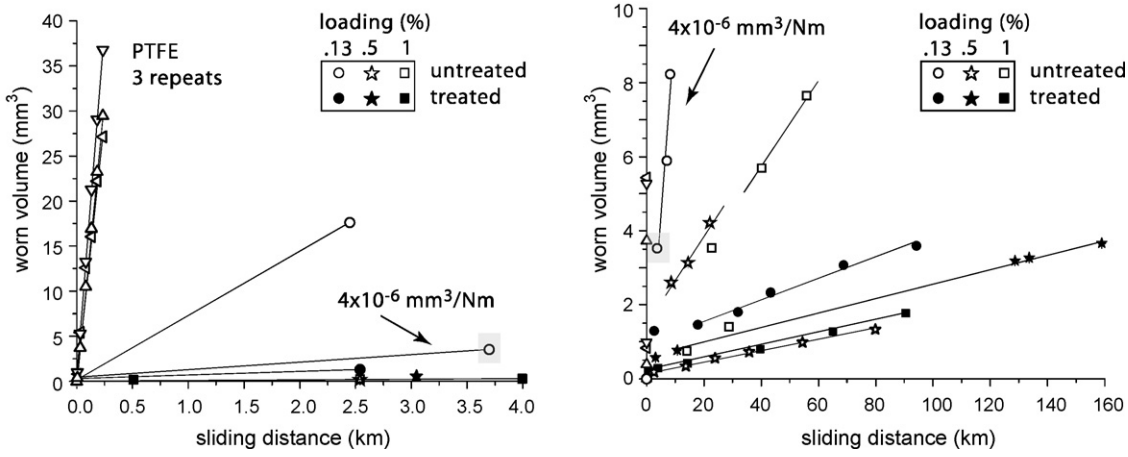

Fig. 2. Worn volume of alumina-PTFE nanocomposites plotted versus sliding distance. Left: the first 4 km of sliding is plotted in order to reveal the contrast between the contrast between the wear behavior of unfilled PTFE and the PTFE nanocomposites. Right: the entore 160 km of data is plotted, but the y-axis is limited to wear volumes below 10 mm^3 in order to elucidate differences among the nanocomposites. The normal load was 250 N, contact pressure was 6.4 MPa and sliding speed was 50.8 mm/s. Confidence intervals representing the experimental uncertainties were smaller than data indicators.

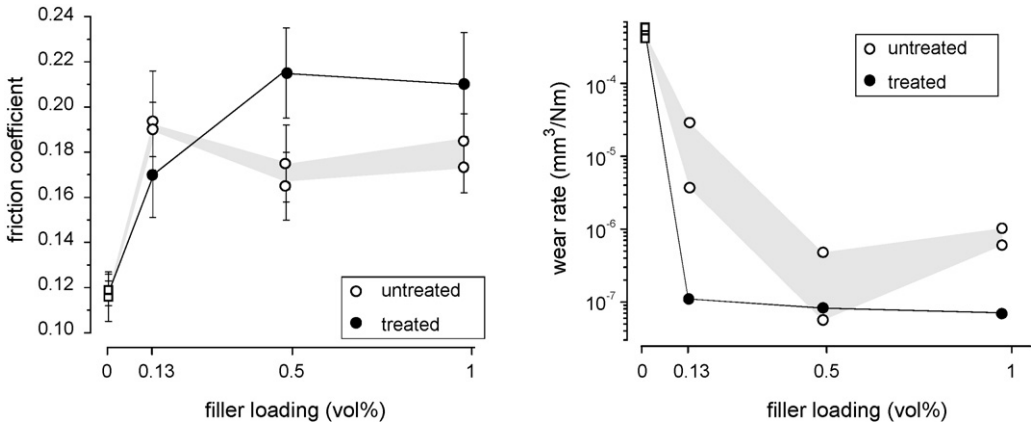

Fig. 3. (Left) Average friction coefficients plotted versus nanoparticle loading. Confidence intervals represent the standard deviation of averaged data collected during the test. The experimental uncertainty is $U(\mu) = 0.005$. (Right) Steady state wear rate plotted versus nanoparticle loading. Confidence intervals representing the experimental uncertainty are smaller than the data.

deviation from randomness is not the defining parameter. Briefly, the method consists of converting transmission electron images of the nanocomposite dispersions into two-dimensional point maps. A Monte-Carlo technique is then used to place a statistically large number of squares of prescribed characteristic length in random locations on the surface. The number of particles within each box is counted, and from this single experiment, a histogram of the number of points per box is collected. The size of unreinforced PTFE, or the particle-free space (PFS), is equal to the largest box for which the most probable number of particles is zero.

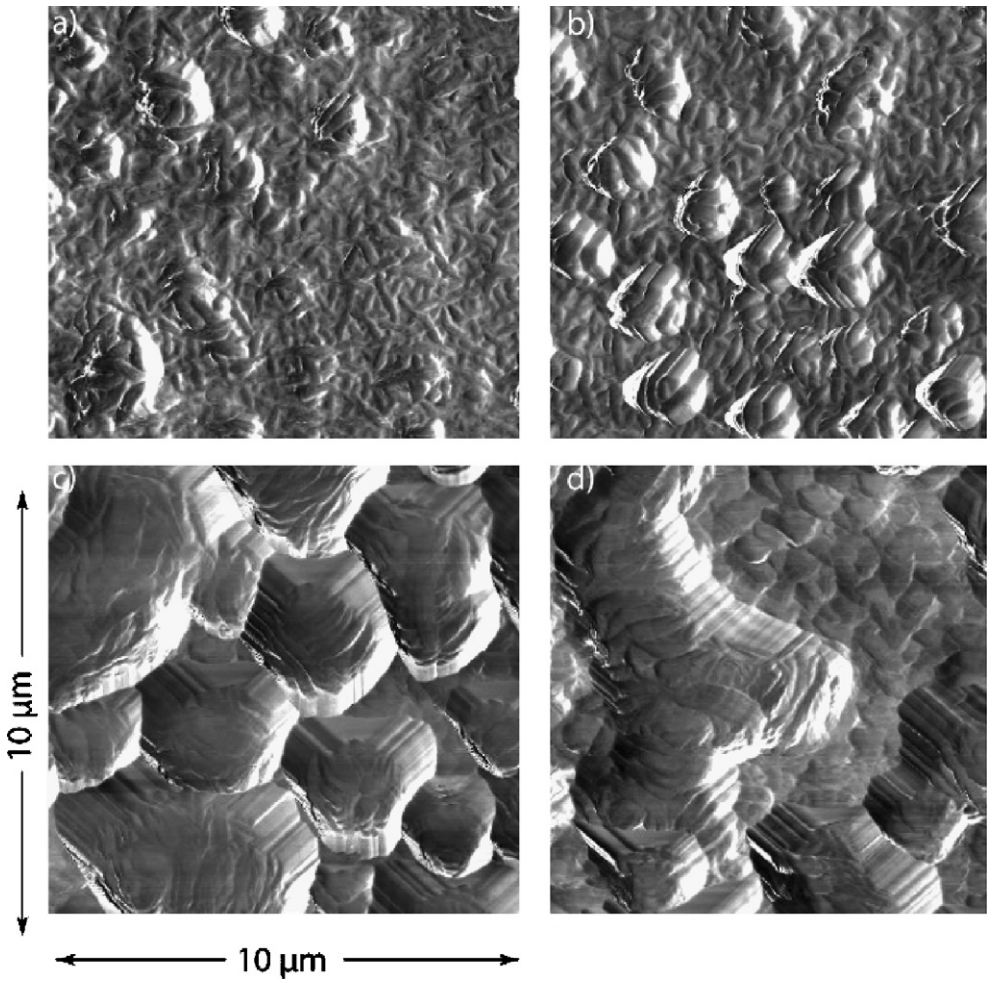

Fig. 4. Intermittent contact atomic force microscopy phase imaging: (a) neat PTFE, (b) 0.5 vol% 40 nm Δ:Γ phase alumina-PTFE, (c) 0.5 vol% 40 nm α phase alumina-PTFE treated with fluorosilane treated nanoparticles, (d) 0.5 vol% 40 nm α phase alumina-PTFE with untreated nanoparticles. The high wear rate ($>10^{-5}$ mm^3/N m) materials (a and b) have similar morphologies that are different than those of low wear rate ($<10^{-6}$ mm^3/N m) materials (c and d).

3. Results

3.1. Tribology

The tribological results of this study are listed in Table 1. Wear rates are expressed in units of 10^{-6} mm^3/N m; 1×10^{-6} mm^3/N m is as a reasonable datum for a wear resistant polymer (e.g. PEEK). The unfilled PTFE samples had an average wear rate of $500 \times 10^{-6} \pm 88 \times 10^{-6}$ mm^3/N m; i.e. they wore at about 500× the rate of a wear resistant polymer. This severe wear of PTFE is well-documented in the literature [1–4]. Despite the trace filler loading, the least wear resistant nanocomposite was still more than 10× more wear resistant than unfilled PTFE. Such large reductions in wear rate give nearly 100% confidence regarding the statistical significance of the wear reduction effect from the incorporation of low loadings of nanoparticles into the PTFE matrix.

The worn volume of the samples is plotted versus the sliding distance in Fig. 2. The plot on the left distinguishes unfilled behaviour from filled behaviour. The unfilled PTFE samples were completely worn down after 300 m, which was less than 2 h of sliding. Some of the nanocomposites, however, required up to two months of testing to produce 1/10th of the worn volume that PTFE generated. A 0.13% nanocomposite with a wear rate of 4×10^{-6} mm^3/N m has been highlight; it demonstrated behaviour comparable to wear resistant engineering polymers like PEEK at a fraction of the friction coefficient. Another noteworthy feature of this graph is the lack of worn volume for many of the samples after 1 km of sliding. Generally, transient wear rates of these soft materials are much higher against the exposed steel counterface [16,28,29]. Once transfer films are initiated, the wear rate is reduced until steady conditions are reached. These materials demonstrated remarkable initial wear resistance and little volume loss during transient conditions.

Some of the nanocomposites had orders of magnitude lower wear rates than materials traditionally considered to be wear resistant, and determination of steady state wear rates required extensive sliding distances. The untreated 0.5 and 1% nanocomposites are significantly more wear resistant than the 0.13% samples (100 times in one case). In general, the untreated samples showed sample to sample variation that is typical of lightly loaded nanocomposites. The treated samples showed extraordinary wear resistance and consistency by comparison. With nearly an order of magnitude difference in the filler content, the worn volumes varied by less than 2×. As filler loading increased, the steady wear rate, transient wear rate (while establishing transfer films) and the transient volume loss all decreased monotonically.

Averages and standard deviations of collected friction coefficients are plotted versus loading on the left of Fig. 3. In general, the addition of nanofillers led to significant increases in the friction coefficients. It should be noted that this trend is likely only relevant for the 50 mm/s sliding speed used here. At 80 mm/s, McElwain et al. [18] showed that similar 2.5% alumina-PTFE nanocomposites and unfilled PTFE both had a friction coefficient of approximately 0.18. We have conducted very preliminary studies with a rotary tribometer which indicated that the nanocomposite friction coefficient is far less speed sensitive than that of the unfilled polymer.

Wear rates are plotted versus filler loading on the right of Fig. 3. The wear rates of the treated samples were more than an order of magnitude lower than other 'optimized' nanocomposites in the literature. Further, they retained these unprecedented levels of wear resistance down to comparably unprecedented loadings; 1/100th the filler loading was required for 10 times the wear resistance found with other nanofillers [13–15]. The untreated samples had higher wear rates in general with sample to samples variability becoming more prominent at low loadings. McElwain found low wear at 2.5% loading of the same materials dispersed

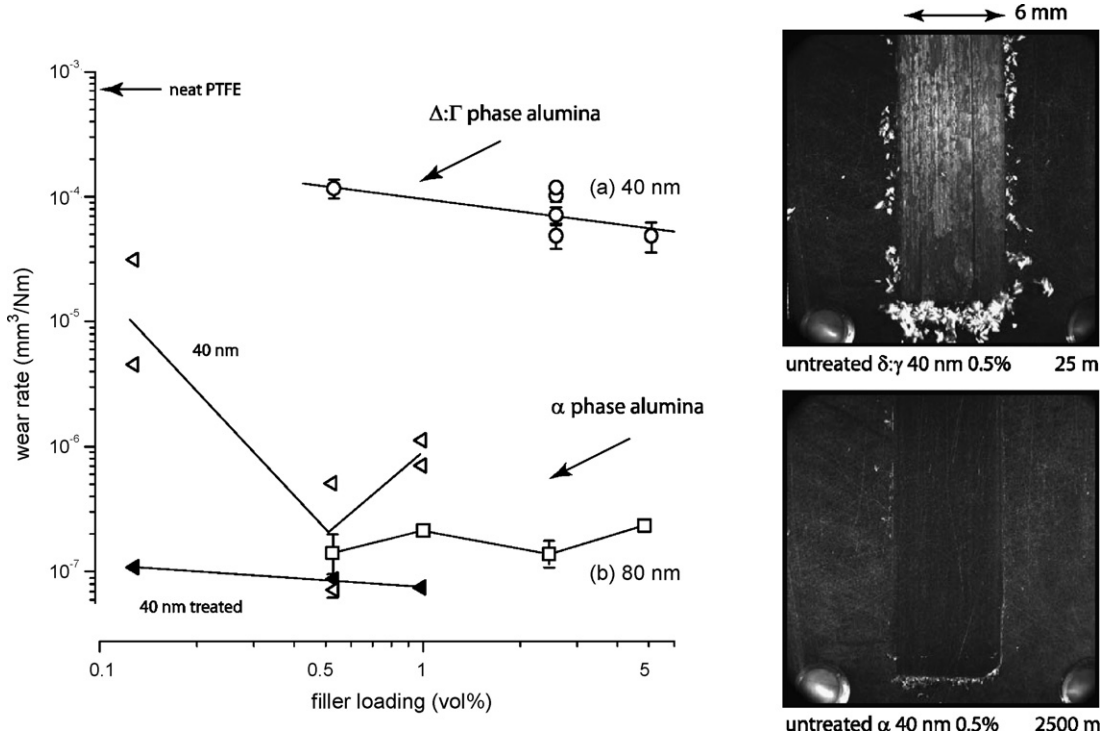

Fig. 5. (Left) Wear rate plotted versus filler loading for identically prepared and tested alumina-PTFE nanocomposites: (a) Burris and Sawyer [16], (b) Burris and Sawyer [17]. The δ:γ phase alumina is consistent with prior literature, while α phase alumina consistently demonstrates drastic improvements in the obtainable wear rate and the loadings needed to achieve high wear resistance. (Right) micrographs showing characteristic transfer films of low wear (bottom) and high wear (top) nanocomposites. High wear materials liberate large debris rapidly and produce thick unstable transfer films. Low wear systems infrequently liberate much smaller debris which promotes very thin and stable transfer films.

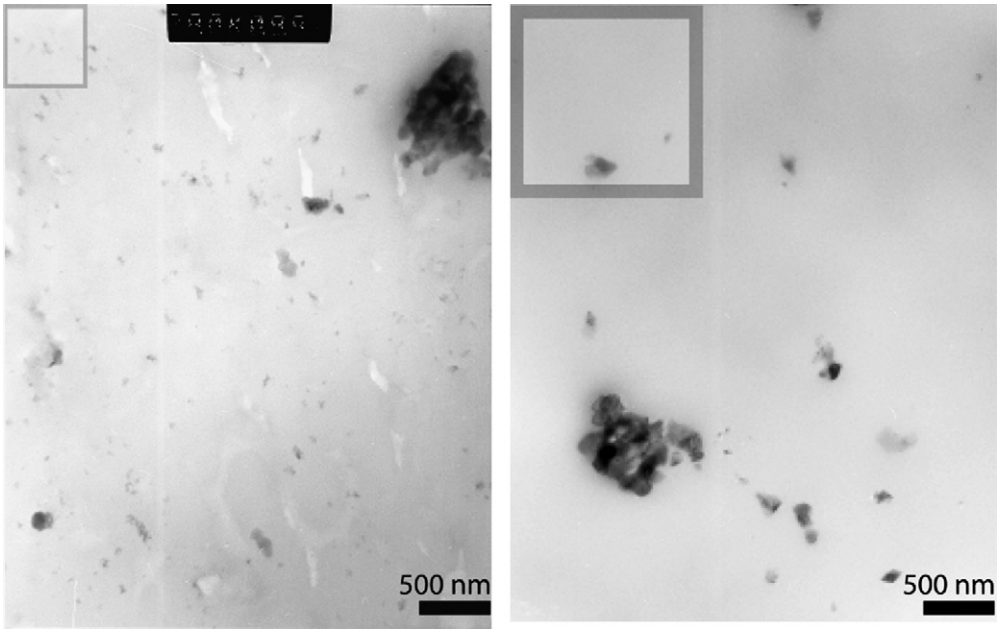

Fig. 6. Transmission electron images (22,000×) of nanoparticle dispersions for 0.5 vol% alumina-PTFE nanocomposites: (left) nanoparticles treated with a fluorosilane treatment; PFS = 540 ± 20 nm, (right) untreated nanoparticles; PFS = 1240 ± 60 nm. Many individually dispersed nanoparticles are observed to segment the PTFE into smaller characteristic regions within treated samples. The boxes indicate the PFS mean plus and minus one standard deviation. Larger characteristic regions of unfilled polymer were observed in untreated samples due to increased clustering of nanoparticles.

with a lower energy rotary dispersion technique. At 0.4%, he found almost no improvement (3× reduction) [6]. These results suggest that wear rate is extremely sensitive to dispersion at low loadings. At a given set of conditions, an increase in particle size, a decrease in loading or an increase in the aggregation of particles increases the characteristic length of unreinforced PTFE. At a critical unreinforced length scale or particle-free space, it is hypothesized that size of unreinforced PTFE exceeds the 'reach' of the nanoparticles' influence on morphology which leads to a composite of high wear and low wear material.

3.2. Morphology

Intermittent-contact atomic force microscopic phase images of unfilled PTFE, 0.5% α phase alumina-PTFE and treated 0.5% α phase alumina-PTFE are shown in Fig. 4. An additional comparison is made to 0.5% δ:γ phase alumina-PTFE which was not found to exhibit significantly improved wear resistance at these loadings [15,16]. While the structures shown here were the predominant structures, the surfaces demonstrated some heterogeneity. Fig. 4(a) shows the unfilled PTFE and bands of lamellar crystals. Fig. 4(b) shows a similar morphology for the high wear rate δ:γ alumina-PTFE. Fig. 4(c) and (d) show very different structures that were much more homogeneous across the entire sample. The α phase alumina induced a coarsened, and more equiaxed crystalline structure in the PTFE and this morphological feature was clearly more homogeneous for the treated sample.

These observations demonstrate correlation between the PTFE wear resistance and morphology; the particles with little influence on PTFE wear also appear to have little impact on the polymer morphology, while wear reducing nanoparticles have a clear effect on PTFE morphology. These results reinforce the hypothesis that the primary role of the nanoparticles is the initiation of a unique wear resistant morphology in the polymer.

3.3. Dispersion

The dispersions of treated and untreated samples were examined to study potential effects of the treatment on dispersion and wear rate. Transmission electron microscopy images of the nanoparticle dispersions of 0.5 vol% treated and as-received alumina-PTFE nanocomposites are shown in Fig. 6. Both samples contained agglomerations that are on the micrometer size scale. In the nanocomposites with untreated alumina, the alumina was only found within large agglomerates and small clusters. In nanocomposites with treated alumina, the nanoparticles were found within agglomerates and individually dispersed. The individually dispersed particles resulted in a clear decrease in the characteristic size of the unreinforced PTFE; this is quantitatively reflected by a significant reduction in the particle-free space from 1240 ± 60 (untreated) to 540 ± 20 (treated). These images, which constitute only about 10^{-12} of the sample volume, give little indication of the global particle distribution. However, they do provide significant evidence that the treatment reduced clustering and the particle-free space, which reduced the loadings needed for low wear and low variability.

4. Discussion

There remain large disconnects in the PTFE nanocomposites literature; while we have demonstrated high wear resistance at low loadings, much of the literature in this area indicates that significantly higher loadings are required for significantly lower wear resistance. The discrepancy is well illustrated by Fig. 5 in which wear rate is plotted versus alumina nanoparticle loading. These samples were processed and tested under the same conditions; the primary variables are alumina size and phase. There is little dependence of wear rate on size, but the dependence of wear rate on phase is striking; δ:γ phase alumina is orders of magnitude less effective than α phase alumina at reducing wear of PTFE at loadings up to 5%. The micrographs on the right of Fig. 5 reveal clear differences in the transfer films and the wear debris size. The differences in sliding distances and debris quantities illustrate dramatically different rates of debris generation. Wear resistant samples develop a brown discoloration at the sliding interface; we have previously shown that this is due to eventual and accumulated defluorination of the PTFE at stable, low wear interfaces [19].

It is clear that the fillers have unique effects on the size and number of debris particles generated, but the mechanisms responsible remain obscure. The results of this study showed correlation to a modified morphology of the PTFE. The inefficient δ:γ phase alumina had little effect on the polymer morphology. It is suggested that the regions of unfilled polymer exceeded the range of the interfacial effects which resulted in high wear rate regions within the nanocomposite. A lingering hypothesis is that ineffective dispersion results in larger regions unreinforced polymer. A 2.5% δ:γ phase alumina sample with poor wear resistance was microtomed and TEM imaged. The dispersion was found to be comparable or even improved compared to α phase alumina-PTFE nanocomposites indicating that the PTFE response to δ:γ particles is either absent or greatly attenuated compared to the response to α alumina. The lack of interaction with PTFE likely leaves only mechanical effects for wear reductions. Tanaka and Kawakami suggested that these particles are too small to interfere with large-scale damage [8]; while δ:γ alumina, ZnO, CNT and TiO_2 have produced very significant wear reductions in PTFE, these mechanical mechanisms are clearly limited and inefficient in comparison to the interfacial mechanisms present with α phase alumina.

The general polymer nanocomposites literature has demonstrated that the nanocomposite properties are critically dependent upon the properties of the nanoparticle surface and the resulting response of the polymer to that surface [10,12,33]. As the size of the particle is reduced to the nanoscale, the modified interfacial regions constitute more considerable fractions of the polymer and bulk properties like wear rate can be dramatically influenced. Numerous authors have observed the direct effects of these nanoscale interactions through changes in the glass transition and degradation temperatures of the polymer matrices [9,34–36]. This study has shown that the surface characteristics of α phase alumina induce a favourable response by the PTFE which manifests into modified morphology and wear rate. The results of this study suggest that the unique morphology of the PTFE, not the nanoparticles, resists the large-scale subsurface deformation processes that the unfilled polymer is susceptible to. For a critical combination of particle size, loading and dispersion, the range of the active interfaces exceeds the characteristic length scale of the unfilled polymer; the entire polymer becomes modified and the wear rate is low. Since the entire matrix has been influenced at the tipping point, improvements to any single parameter (e.g. increase loading for constant particle size and dispersion) have little effect. This trend is illustrated by the 80 nm alumina samples of Fig. 5. If changes in size loading or dispersion increase the characteristic length scale of the unfilled polymer regions (poor dispersion, large size or low loading), regions of high wear unmodified PTFE weigh heavily on the composite wear rate. This is supported by the report by McElwain [6] that the particles were no longer effective at 0.4% using rotary dispersion, and the low loading variability found here using jet-mill dispersion of untreated particles. Following nanoparticle treatment, dispersion improved and wear resistance was extended to trace filler loadings.

5. Conclusions

This paper reports on the effectiveness of a nanoparticle surface treatment on the wear reductions in lightly loaded PTFE-alumina nanocomposites. The Fluorosilane treated particles maintained unique wear reduction capabilities down to unprecedented filler loadings (0.13%); other nanomaterials require 100 times this loadings for 1/10th the wear resistance. The findings suggest that the properties of this particular particle surface induce a unique and wear resistant PTFE morphology, while the dispersion of these particles governs the efficiency with which the morphology is converted.

- Wear reductions with 0.13% loading untreated alumina were significant, varying from 10–100×. The results confirmed that α phase alumina is significantly more effective at reducing wear of PTFE than other materials in the literature, which include δ:γ phase alumina, ZnO, TiO_2, SWCNT.
- Treated nanoparticles produced unprecedented wear resistance in PTFE down to 0.13% loading; wear was improved 6000–10,000× from 0.13 to 1% loading.
- Treated and untreated α phase alumina particles induced an altered PTFE morphology; the morphology was more uniformly modified by treated nanoparticles. This morphology modification correlated with the wear resistance of the sample.
- TEM observations showed individually dispersed treated particles; clustering of untreated particles led to larger characteristic regions of unfilled polymer higher wear rates and increased variability at low loadings. The surface treatment and improved dispersion reduced wear rates and variability, particularly at the low loadings of interest.

Acknowledgements

This material is based upon an AFOSR-MURI grant FA9550-04-1-0367. Any opinions, findings, and conclusions or recommendations expressed in this material are those of the authors and do not necessarily reflect the views of the Air Force Office of Scientific Research.

References

[1] S. Bahadur, D. Tabor, The wear of filled polytetrafluoroethylene, Wear 98 (1984) 1–13.
[2] T. Blanchet, F. Kennedy, Sliding wear mechanism of polytetrafluoroethylene (PTFE) and PTFE composites, Wear 153 (1992) 229–243.
[3] K. Makinson, D. Tabor, Friction + transfer of polytetrafluoroethylene, Nature 201 (1964) 464.
[4] K. Tananka, Y. Uchiyama, S. Toyooka, Mechanism of wear of polytetrafluoroethylene, Wear 23 (1973) 153–172.
[5] J.K. Lancaster, Polymer-based bearing materials–role of fillers and fiber reinforcement in wear, Wear 22 (1972) 412.
[6] S. McElwain, Wear resistant PTFE Composites via Nano-Scale Particles. Master's Thesis, Rensselaer Polytechnic Institute, Troy, New York, 2006.
[7] N. Sung, N. Suh, Effect of fiber orientation on friction and wear of fiber reinforced polymeric composites, Wear 53 (1979) 129–141.
[8] K. Tanaka, S. Kawakami, Effect of various fillers on the friction and wear of polytetrafluoroethylene-based composites, Wear 79 (1982) 221–234.
[9] B. Ash, L. Schadler, R. Siegel, Glass transition behavior of alumina/polymethylmethacrylate nanocomposites, Materials Letters 55 (2002) 83–87.
[10] A. Eitan, F. Fisher, R. Andrews, L. Brinson, L. Schadler, Reinforcement Mechanisms in MWCNT-filled polycarbonate, Composites Science and Technology 66 (2006) 1162–1173.
[11] C. Ng, L. Schadler, R. Siegel, Synthesis and mechanical properties of TiO_2-epoxy nanocomposites, Nanostructured Materials 12 (1999) 507–510.
[12] A. Zhu, S. Sternstein, Nonlinear viscoelasticity of nanofilled polymers: interfaces, chain statistics and properties recovery kinetics, Composites Science and Technology 63 (2003) 1113–1126.
[13] W. Chen, F. Li, G. Han, J. Xia, L. Wang, J. Tu, Z. Xu, Tribological behavior of carbon-nanotube-filled PTFE composites, Tribology Letters 15 (2003) 275–278.
[14] F. Li, K. Hu, J. Li, B. Zhao, The friction and wear characteristics of nanometer ZnO filled polytetrafluoroethylene, Wear 249 (2001) 877–882.
[15] W. Sawyer, K. Freudenberg, P. Bhimaraj, L. Schadler, A Study on the friction and wear behavior of PTFE filled with alumina nanoparticles, Wear 254 (2003) 573–580.
[16] D. Burris, W. Sawyer, Tribological sensitivity of PTFE/alumina nanocomposites to a range of traditional surface finishes, Tribology Transactions 48 (2005) 147–153.
[17] D. Burris, W. Sawyer, Improved wear resistance in alumina-ptfe nanocomposites with irregular shaped nanoparticles, Wear 260 (2006) 915–918.
[18] S. McElwain, T. Blanchet, L. Schadler, W. Sawyer, Effect of particle size on the wear resistance of alumina-filled PTFE micro- and nanocomposites, Tribology Transactions 51 (2008) 247–253.
[19] D. Burris, K. Santos, S. Lewis, X. Liu, S. Perry, T. Blanchet, L. Schadler, W. Sawyer, Polytetrafluoroethylene matrix nanocomposites for tribological applications,

in: K. Friedrich, A. Schlarb (Eds.), Tribology of Polymeric Nanocomposites, 2008, pp. 403–435.
[20] P. Bhimaraj, D. Burris, J. Action, W. Sawyer, C. Toney, R. Siegel, L. Schadler, Effect of matrix morphology on the wear and friction behavior of alumina nanoparticle/poly(ethylene) terephthalate composites, Wear 258 (2005) 1437–1443.
[21] F. Kuchta, P. Lemstra, A. Kellar, L. Batenburg, B. LF, H. Fisher, Materials with improved properties from polymer-ceramic-nanocomposites, Material Research Society Symposium Proceedings 576 (1999) 363–368.
[22] D. Ma, Y. Akpalu, Y. Li, R. Siegel, L. Schadler, Effect of titania nanoparticles on the morphology of low density polyethylene, Journal of Polymer Science Part B-Polymer Physics 43 (2005) 488–497.
[23] E. Petrovicova, R. Knight, L. Schadler, T. Twardowski, Nylon 11/silica nanocomposite coatings applied by the HVOF process. II. Mechanical and barrier properties, Journal of Applied Polymer Science 78 (2000) 2272–2289.
[24] E. Petrovicova, R. Knight, L. Schadler, T. Twardowski, Nylon 11/silica nanocomposite coatings applied by the HVOF process. I. Microstructure and morphology, Journal of Applied Polymer Science 77 (2000) 1684–1699.
[25] H. Yang, P. Bhimaraj, R. Siegel, L. Schadler, Crystal growth in alumina/poly(ethylen terephthalate) nanocomposite films, Journal of Polymer Science Part B: Polymer Physics 106 (2007) 4233–4240.
[26] K. Yang, Q. Yang, G. Li, Y. Sun, D. Feng, Morphology and mechanical properties of polypropylene/calcium carbonate nanocomposites, Materials Letters 60 (2006) 805–809.
[27] D.L. Burris, Effects of nanoparticles on the wear resistance of polytetrafluoroethylene, Doctoral Thesis, University of Florida, Gainesville Florida, 2007.
[28] D.L. Burris, B. Boesl, G.R. Bourne, W.G. Sawyer, Polymeric nanocomposites for tribological applications, Macromolecular Materials and Engineering 292 (2007) 387–402.
[29] S. Bahadur, The development of transfer layers and their role in polymer tribology, Wear 245 (2000) 92–99.
[30] T. Schmitz, J. Action, D. Burris, J. Ziegert, W. Sawyer, Wear-rate uncertainty analysis, Journal of Tribology –Transactions of the ASME 126 (2004) 802–808.
[31] T. Schmitz, J. Action, J. Ziegert, W. Sawyer, The difficulty of measuring low friction: uncertainty analysis for friction coefficient measurements, Journal of Tribology –Transactions of the ASME 127 (2005) 673–678.
[32] P. Karnezis, G. Durrant, B. Cantor, Characterization of reinforcement distribution in cast Al-Alloy/SiC_p composites, Materials Characterization 40 (1998) 97–109.
[33] D. Wagner, R. Vaia, Nanocomposites: issues at the interface, Materials Today (2004) 38–42.
[34] T. Agag, T. Koga, T. Takeichi, Studies on thermal and mechanical properties of polyimide–clay nanocomposites, Polymer 42 (2001) 3399–3408.
[35] D. Ratna, S. Divekar, A. Samui, B. Chakraborty, A. Banthia, Poly(ethylene oxide)/clay nanocomposite: thermomechanical properties and morphology, Polymer 47 (2006) 4068–4074.
[36] A. Yasmin, J. Luo, J. Abot, I. Daniel, Mechanical and thermal behavior of clay/epoxy nanocomposites, Composite Science and Technology 66 (2006) 2415–2422.